

The Coulomb bridge function and the Pair-distribution functions of the 2-dimensional electron liquid in the quantum regime.

M.W.C. Dharma-wardana

National Research Council of Canada, Ottawa, Ontario, Canada, K1A 0R6 *

(Dated: October 26, 2010)

The electron-electron pair distribution functions (PDF) of the 2-D electron fluid (2DEF) in the quantum regime (at $T=0$) are calculated using a classical-map-hyper-netted-chain (CHNC) scheme and compared with currently available Quantum Monte-Carlo (QMC) simulations in the coupling range $r_s=1$ to 50. We iteratively extract the bridge function of the “equivalent” classical 2-D liquid in the quantum regime. These bridge functions $B(r)$ are relatively insensitive to spin-polarization effects. The structure of the bridge functions changes significantly for $r_s > 6$, suggesting the onset of strongly correlated clusters. The new $B(r)$, appropriate for the long-range Coulomb potential, can be used to replace the hard-sphere $B(r)$ previously used in these calculations. They provide accurate classical representations of the QMC-PDFs even at very strong coupling, and probably at finite- T near $T = 0$.

PACS numbers: PACS Numbers: 05.30.Fk, 71.10.+x, 71.45.Gm

I. INTRODUCTION

The pair-distribution functions (PDFs) of strongly-coupled electron fluids contain all the physical information associated with the ground-state static properties of such systems. Exchange-correlation energies, phase-transitions, and Fermi-liquid parameters like the effective mass m^* , and the spin-susceptibility enhancement (g^*) can all be evaluated from the PDFs, as discussed below. The static local-field corrections to the response functions can also be addressed via these PDFs.

The PDFs are usually determined by quantum Monte-Carlo (QMC) simulations, since standard many-body methods become unreliable for densities where the electron-sphere radius r_s exceeds unity. The r_s parameter is also the ratio of the mean Coulomb energy and the Fermi energy, and hence is a measure of the coupling strength. QMC simulations for the 2D electron system were first published by Tanatar and Ceperley¹, and more recently by Attaccalite et al.², and by Drummond and Needs³. A transition from the paramagnetic state to the ferromagnetic phase was predicted to occur at $r_s \sim 26$ by Attaccalite et al., while weak-coupling theories (Hartree-Fock, RPA) predicted such transitions already at very low values of r_s . In contrast, Tanatar and Ceperley, as well as the most recent QMC work by Drummond et al., find no such phase transition, where the ferromagnetic state is very close in energy, but the paramagnetic state remains the ground state. Indeed, direct comparisons of the QMC-PDFs of Attaccalite et al., with the more accurate PDFs of Drummond et al., show slight differences which show the need to be cautious about undue claims of final accuracy.

QMC methods have also been used to calculate Fermi-liquid parameters² like m^* and g^* , but these, and especially the m^* calculation⁴ may require further effort before a consensus is reached.

Besides QMC, one other method⁵ available for the calculation of PDFs of quantum (e.g., electron) fluids

at arbitrary coupling, temperature and spin polarization is based on considering a classical charged fluid at an assigned classical-fluid temperature T_{cf} , selected to reproduce the correct correlation energy of the quantum fluid which has two spin species α, β . The non-interacting PDFs $g_{\alpha,\beta}^0(r)$ of the classical charged fluid are formulated to agree with the analytically known non-interacting $g_{\alpha,\beta}^0(r)$ of the quantum fluid. This is done by introducing an effective potential known as the Pauli exclusion potential $P_{\alpha,\beta}$ to exactly reproduce the Fermi hole in the parallel-spin $g^0(r)$. Once an “equivalent” classical map of the quantum fluid is constructed, its PDFs are obtained using a classical integral equation, namely, the hyper-netted-chain (HNC) equation modified to include bridge corrections. This classical-map hyper-netted chain procedure was called the CHNC, and we showed that the method was surprisingly accurate. The classical-fluid temperature of the quantum fluid at $T = 0$ was called the “quantum temperature” T_q . In fact, using *only* the correlation energies tabulated by Tanatar and Ceperley as the inputs, we constructed the effective quantum temperature T_q as a function of r_s , and showed that accurate PDFs of the quantum fluid could be calculated at arbitrary r_s via the classical map⁵. Balutay and Tanatar⁶ also presented a closely similar temperature map. The advantage of the CHNC approach is that it is numerically very simple, and makes many properties (spin-dependent properties, Fermi-liquid parameters, local-field corrections, finite- T results, etc.) easily computable with negligible effort. Thus the product m^*g^* can be evaluated⁷ from the second derivative of the correlation energy with respect to the the spin-polarization ζ . The effective mass m^* can be obtained⁷ from the second density-derivative of the free energy which can be evaluated from the temperature-dependent PDFs.

However, the classical map of the 2D- electron fluid leads to a Coulomb fluid for which the simple HNC is inadequate. The irreducible three-body and higher-order contributions which are lumped into the bridge term

$B_{\alpha,\beta}(r)$ are very difficult to calculate directly. The need for bridge functions appears in many areas in the theory of Coulomb systems⁸. Hence, as is customary⁹, in our earlier work we used a hard-disk model, based on solutions of the Percus-Yevik equation¹⁰. However, the availability of an extensive set of QMC-generated PDFs for the 2D-electron fluid presents the possibility of extracting accurate Coulomb-adapted bridge functions $B(r)$. These are implicit functions of the PDFs themselves¹¹. Thus, in this paper we present an iterative procedure for extracting the 2D-bridge functions appropriate to a classical Coulomb fluid at a given r_s , and at the effective classical-fluid temperature T_{cf} , and yielding the *quantum* PDF at the given r_s and at $T = 0$.

II. HNC AND CHNC METHODS

The HNC equation¹² and its generalizations, coupled with the Ornstein-Zernike equation have lead to very accurate results for classical charged-particle interactions. In the following we use indices i, j which could be spin indices or other species-identifying indices. The exact equations for the PDFs are of the form:

$$g_{ij}(r) = e^{-\beta_{cf}\phi_{ij}(r) + N_{ij}(r) + B_{ij}(r)} \quad (1)$$

$$N_{ij} = h_{ij}(r) - c_{ij}(r) \quad (2)$$

$$h_{ij}(r) = g_{ij}(r) - 1 \quad (3)$$

Here $\phi_{ij}(r)$ is the pair potential between the species i, j , and $N_{ij}(r)$ is the nodal function, while $c_{ij}(r)$ is the direct correlation function connected to h_{ij} by the Ornstein-Zernike (O-Z) equation. The pair potential $\phi_{ij}(r)$ is the sum of a diffraction corrected Coulomb potential and the Pauli exclusion potential (see Eq. 1-2 , ref⁵).

If the bridge function $B_{ij}(r)$ were set to zero we have the HNC approximation, adequate for systems where the kinetic energy dominates strongly over the potential energy. The bridge function brings in many-body cluster interactions beyond the diagrams of the hyper-netted chain expansion. A systematic investigation of the 3-D one-component plasma was given many years ago by Lado et al⁹. As the bridge interactions involve many-internal interactions (within the cluster) averaged over, they are somewhat insensitive to the exact form of the pair-interactions, and their spin-states. Thus it was shown¹⁰ that the analytically available Percus-Yevik hard-sphere bridge function could be used for most fluids, to closely reproduce the Monte-Carlo PDFs available at the time. The hard-sphere radius of the model bridge function was in effect an optimization parameter in such approaches to liquid structure.

The PDFs of the classical 2D electron fluid became relevant to 2D quantum fluids when Laughlin¹³ introduces his plasma mapping of 2D fractional-quantum Hall (FQH) fluids to classical plasmas. The use of a suitable bridge function was found to be essential if high accuracy was to be obtained via the plasma map¹⁴ for the

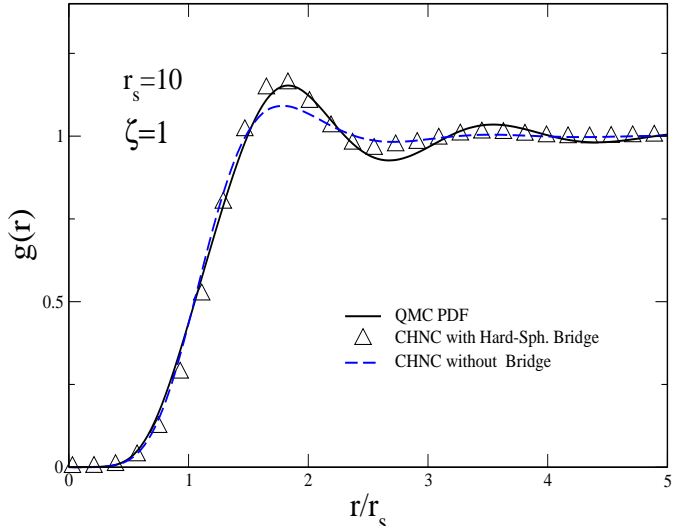


FIG. 1: (Online color) The QMC pair-distribution function of a fully spin polarized ($\zeta = 1$) electron fluid at $r_s = 10, T = 0$ is compared with those calculated from CHNC using a hard-sphere bridge function and with no bridge function what so ever

hierarchy of FQH states. The temperature of the classical fluid in Laughlin's classical map is directly related to the filling factor, via the form of the many-body wavefunction proposed by Laughlin (Laughlin used a simple HNC without bridge corrections). There is no external magnetic field in the 2D systems studied here. It turns out that the temperature of the classical charged fluid whose PDF agrees with the electron (quantum) fluid at $T = 0$ can be expressed⁵ as a function of the density parameter r_s .

We found⁵ that the use of hard-sphere model bridge functions gave good agreement around the first peak of the PDFs, while the more distant oscillations were weaker than those in the QMC-PDFs. The PDF of the fully spin-polarized $T = 0$ electron fluid at $r_s = 10$, calculated using CHNC without bridge, and CHNC with a hard-sphere bridge function⁵, and the bench-mark QMC-PDF are shown in Fig. 1.

The bridge function $B(r)$ is a function of the PDFs themselves, and hence their extraction from QMC simulation results is by no means obvious. However, given a choice for the effective pair potential and classical-fluid temperature implicit in the CHNC $\beta\phi(r)_{ij}$, and the assumed applicability of the modified-HNC equation and the O-Z equation, a bridge function can be evaluated from the QMC- $g(r)$. This evaluation requires separating out the long-range tails of the pair-potentials, direct correlations etc., in r - and k -space, using numerical Fourier transforms for the short range parts, analytical formulae for the long ranges parts and reassembling the results in r - and k -space. Since these mathematical machinery are already available in the algorithms for the CHNC, we present here a simple iterative scheme equivalent to the

above, but using the CHNC code itself.

The $B(r)$ functions obtained from such a procedure, together with the $\beta\phi(r)$ of CHNC present a complete, accurate, classical representation of the quantum PDFs obtained by QMC. It is hoped that such bridge functions and classical maps can then be used in regimes where QMC simulations are not possible or easily available, as discussed below.

III. EXTRACTION OF THE BRIDGE FUNCTION FROM QMC DATA

Given a density $n = 1/(\pi r_s^2)$ specified by an r_s value, the target QMC-PDFs that we use are those of Attaccalite et al., as parametrized by Gori-Giorgi et al.¹⁵. We drop the species indices i, j except when required, and indicate the PDFs from QMC and CHNC by $g(r)$ and $g_{chnc}(r)$. Given the hypothesis that the QMC-PDFs can be represented by classical forms, a nodal function and bridge function corresponding to the given target $g(r)$ should exist. Thus the QMC and the CHNC PDFs satisfy

$$\log [g(r)] = -\beta\phi(r) + N(r) + B(r) \quad (4)$$

Both $N(r)$ and $B(r)$ are implicit functions of $g(r)$. However, all the terms in the CHNC form

$$\log [g_{chnc}(r)] = -\beta\phi(r) + N_{chnc}(r) + B_{chnc}(r) \quad (5)$$

are known. Also, it has been found from previous comparisons⁵ of $g(r)$ and $g_{chnc}(r)$ that they agree closely, even when $B_{chnc}(r)$ was taken from a hard-disk model. Hence we assume that $N(r)$ can be replaced by N_{chnc} as a first approximation. Then we easily obtain an initial estimate of the bridge function contained in the QMC-PDF.

$$B(r) = \log [g(r)] - \log [g_{chnc}(r)] + B_{chnc}(r) \quad (6)$$

Thus, starting from the hard-sphere model of $B_{chnc}(r)$ we obtain a standard mixing procedure to construct a new $B_{chnc}(r)$, and hence a new g_{chnc} , and so on. In the small- r region the value of $g(r)$ becomes negligibly small and hence the extraction of the difference between two logarithms becomes numerically unsatisfactory. However, as may be surmised from Eq. 6, the calculated $g(r)$ are found to be insensitive to the form of $B(r)$ for $r < r_s$. Thus even a simple polynomial extrapolation (connecting the $r/r_s < 1$ region with, say the region $1 < r/r_s < 1.5$) or the hard-sphere model itself may be used. The iterative procedure is even insensitive to slight discontinuities at the connection point (although of course, discontinuities should be avoided). These bridge functions will be called “Coulomb bridge functions”, to distinguish them from the hard-sphere bridge functions $B_{HS}(r)$.

The extraction procedure for the Coulomb bridge functions $B_{i,j}(r)$ from the QMC-PDFs, i.e., $g_{ij}(r)$ is found to

be very efficient, and the iterative inclusion of the extracted bridge functions leads to rapid convergence in reproducing the target $g_{ij}(r)$. It is easiest to consider a fully spin-polarized (i.e., $\zeta = 1$) electron fluid as it is a one-component system, with just one bridge function. A set of bridge functions for a range of r_s values which reproduce the QMC pair-distribution functions at $\zeta = 1$ when used in CHNC are shown in Fig. 2. It is found that as r_s increases from 0.3 (not shown) to unity, the $B(r)$ remains more or less unchanged. From then onwards, esp. after $r_s = 3$, the development of the first peak in the PDF produces an oscillatory structure in $B(r)$. This trend continues till about $r_s = 6$. However, now the deepening of the second trough in the PDF leads to a complete qualitative change in the the form of the bridge function, as seen from the panel (b) of Fig. 2. The new deep trough seen near $x = r/r_s \sim 3$ is already there as a weak trough in the moderately coupled fluids of panel (a). In panel (a), the deep trough is in the $r/r_s < 1$ region and it is not of much importance in the HNC equation. In panel (b), when the deep trough near $x \sim 3$ develops, the small x region rises rather steeply. But this rise has only a small numerical significance in the HNC, since the pair potential and the Pauli potential become very large and dominant for small x . In contrast, the structure in $B(r)$ for larger x becomes significant, as the pair-potential effects fall off with increasing x . These results show that the short-range structure of the fluid undergoes significant and subtle changes in the regime $r_s > 6$. Previous studies of the local-field corrections to the response function of the 2D electron liquid had unraveled interesting characteristics^{16,17} which may well be related to the onset of strongly correlated clusters for $r_s > 6$.

Another system which effectively reduces to a one-component system is the paramagnetic electron fluid ($\zeta = 0$) with equal amounts of up-spin, and down-spin species. As a test of spin insensitivity, we can use the bridge functions determined from the $\zeta = 1$ case for the $\zeta = 0$ case and see if the CHNC-PDFs reproduce the QMC-PDFs. This is in fact very nearly the case, showing that the spin-polarization dependence of $B(r)$ is very small. This also shows that, if desired, one may introduce just one bridge function $B(r, \zeta)$ for all i, j components, where the latter is based on linearly interpolating between $B(r, \zeta = 1)$ and $B(r, \zeta = 0)$, since they are very similar. The differences are found in the near $r \sim r_s$ region close to the first peak, where the Pauli-exclusion effects, diffraction effects etc., are comparable to the Coulomb repulsion effects (see the discussion of Fig. 3).

IV. DISCUSSION

Currently, the most sophisticated QMC calculations for the quantum 2D electron liquid are those of Drummond et al. In practice, the differences between those of Drummond et al., and those of Attaccalite et al., are

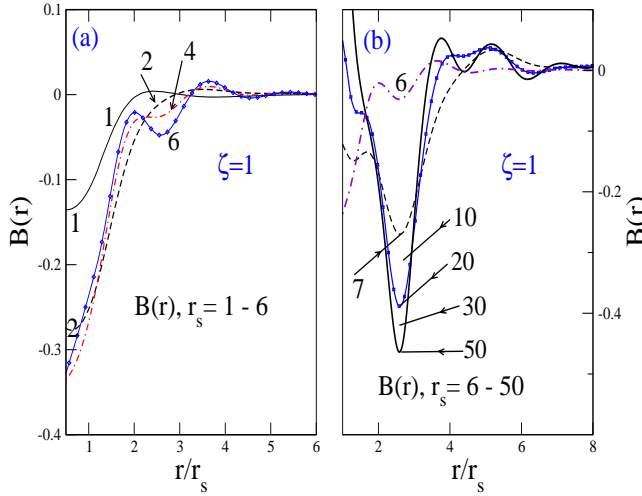


FIG. 2: (Online color) The 2D Coulomb bridge functions needed for a classical description of the pair-distribution function of a fully spin-polarized ($\zeta = 1$) 2D electron fluid, for $r_s = 1$ to 50. Panel (a) shows the weak to moderately coupled regime. Panel (b) shows that the nature of the $B(r)$ changes rapidly near $r_s = 6$ and $r_s = 7$, when the second trough in the PDF begins to develop. The PDFs are insensitive to the behaviour of these functions for $r/r_s \ll \sim 1.3$.

irrelevant except for dealing with very small energy differences indicative of a phase transition from the paramagnetic to the ferromagnetic state. The presence or absence of a ferromagnetic transition would also modify the predictions regarding the enhancement of g^* . The lack of such a transition in the results of Drummond et al., further illustrate the difficulties inherent in assuming that a given set of QMC data are essentially the definitive result. Given the very slight energy differences between the two phases, any technical improvements can modify the conclusions. Since CHNC is based on using some of the QMC data as inputs, and then applying CHNC to other instances, the conclusions of CHNC also get modified as the input QMC data are modified. Thus, in our study of the two-valley 2D electron gas¹⁸ found in Si metal-oxide field-effect transistors (MOSFETs), we used hard-sphere bridge functions, and the classical-fluid temperatures based on the QMC correlation energies of Tanatar and Ceperley as inputs to the CHNC. It was found that the two-valley systems becomes critical at sufficiently high r_s values, when the effective mass and the spin susceptibility become very large. This property is no longer found to be the case when more accurate bridge functions are used.

The pair distribution functions calculated from CHNC using the bridge functions extracted from the Gori-Giorgi et al. fit to the Attaccalite $g(r)$ are, of course, essentially identical to the target $g(r)$. Thus a comparison of CHNC- $g(r)$ using the fitted $B(r)$ is a check on our fitting process as well as an indirect comparison of Refs.² and³. It also enables us to check on the applicability of the $B(r)$ obtained from the polarized-2D system for

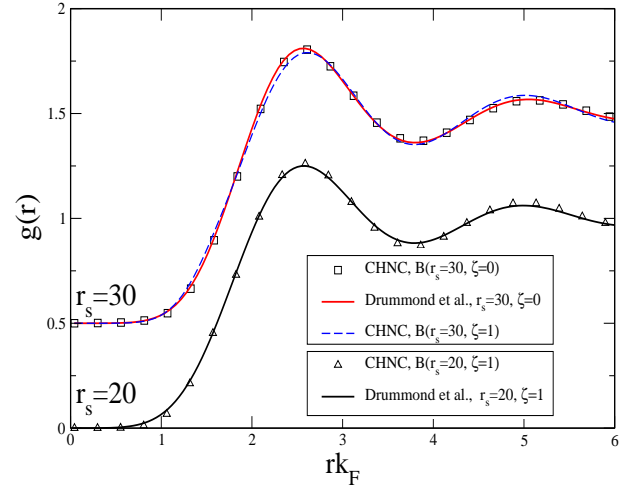


FIG. 3: (Online color) A comparison of the 2D electron-liquid PDFs of Drummond et al.³ with those obtained from the CHNC, using the bridge functions iterated from Eq. 6. In the case of $r_s = 30$, the Drummond et al. data are for $\zeta = 0$, and the effect of using the $\zeta = 1$ bridge function on the PDF (dashes) in CHNC instead of the correct $B(r)$ at $\zeta = 0$ is also shown (PDF, Boxes). The PDFs at $r_s = 30$ have been displaced upwards for clarity.

predictions on the unpolarized system. In fig. 3 we compare CHNC- $g(r)$ with numerical data from Drummond et al.¹⁹, for $r_s = 20, \zeta = 1$, and $r_s = 30, \zeta = 0$. In the latter case, we have also calculated the CHNC PDFs using the appropriate bridge function $B(r, \zeta = 0)$, and also the inappropriate $B(r, \zeta = 1)$ to display the relative insensitivity of the PDF to any spin-polarization dependence in $B(r)$.

It should also be noted that we have not modified the quantum temperature T_q of the classical map given in Ref.⁵ in extracting the bridge functions. In the classical map of Balutay et al., a pure-HNC procedure and a different T_q were used. If it were extended to include the bridge terms, qualitatively very similar results are obtained for the bridge functions which are now slightly different functions.

Once a family of bridge functions for each r_s and T_q is obtained, the $g(r)$ for each r_s as well as all the smaller r_s data are used in the adiabatic-connection formula for the correlation energy E_c . Then the QMC value of E_c will be accurately recovered, and hence we need not revise the preset quantum temperature T_q that was used in the classical map. That is, given a T_q of a classical map of the CHNC type, the use of the Coulomb bridge function based on that T_q instead of the original bridge functions used when forming the T_q , does not require any refitting the T_q . This is a very convenient conservation property for implementing CHNC calculations with improved bridge functions.

The advantage of the CHNC procedure over those of QMC is its simplicity of implementation, as well as its easy applicability to finite- T , finite- ζ situations.

Thus CHNC studies of multi-valley systems (e.g., Si-MOSFETs), nanostructures etc., can be attempted. Finite- T studies become possible if the $B(r)$ remain valid even for finite- T , at least in the near $T = 0$ region. An estimate of the transferability of the $T = 0$ bridge functions to finite- T may be obtained by noting that temperature acts to level out the oscillations in the PDFs, while the $B(r)$ attempts to sharpen the oscillations.

Some years ago we showed²⁰ that very interesting spin-dependent effects arise in the $T = 0$ to $T = E_F$ region due to the interplay of spin, onset of partial degeneracy, Coulomb correlations and temperature effects. Those studies were carried out with the hard-sphere bridge functions available at that time. Such temperature-dependent studies are still beyond the reach of QMC methods. The accuracy of those earlier $B(r)_{HS}$ -based

studies at finite- T can now be further examined using the new bridge functions.

Finite temperature studies of the free energy of the 2D gas as a function of density and spin polarization can also be used to determine Fermi-liquid parameters like the effective mass^{4,21} and the spin susceptibility. In CHNC we directly determine m^* from the second density derivative of the excess free energy with respect to the density⁷. Thus, the availability of these new Coulomb bridge functions which accurately describe the $T = 0$ PDFs provide greater confidence in the results that may be obtained for the Fermi-liquid parameters in future studies.

In conclusion, we have presented an *accurate classical representation* of the pair-distribution functions of the quantum 2D electron fluid at $T = 0$, for arbitrarily strong coupling and arbitrary spin polarizations.

^{*} Email address: chandre.dharma-wardana@nrc-cnrc.gc.ca
¹ B. Tanatar and D. M. Ceperley, Phys. Rev. B **39**, 5005 (1989)
² C. Attaccalite, S. Moroni, P. Gori-Giorgi, and G.B. Bachelet, Phys. Rev. Lett. **88**, 256601 (2002)
³ N. D. Drummond and R. J. Needs, Phys. Rev. B **79**, 085414 (2009)
⁴ N. D. Drummond and R. J. Needs, Phys. Rev. B **80**, 245104 (2009)
⁵ F. Perrot and M. W. C. Dharma-wardana, Phys. Rev. Lett. **87**, 206404 (2001); M. W. C. Dharma-wardana and F. Perrot, *Ibid.* **84**, 959 (2000)
⁶ C. Bulutay and B. Tanatar, Phys. Rev. B **65**, 195116 (2002)
⁷ M. W. C. Dharma-wardana and François Perrot, Phys. Rev. B, **72**, 125339 (2005)
⁸ J. Wrighton, J. W. Dufty, H. Kahlert, and M. Bonitz, arXiv:0909.0775.
⁹ F. Lado, S. M. Foiles and N. W. Ashcroft, Phys. Rev. A, **28**, 2374 (1983) Y. Rosenfeld, Phys. Rev. A **35**, 938 (1987)
¹⁰ Y. Rosenfeld, Phys. Rev. A **42**, 5978 (1990), M. Baus and J.-P. Hansen, J. Phys. C: Solid State Phys. **19**, L463 (1986)
¹¹ P.D. Poll, N.W. Ashcroft, and H.E. DeWitt, Phys. Rev. A

37, 1672 (1988)
¹² J. M. J. van Leeuwen, J. Gröneveld, J. de Boer, Physica **25**, 792 (1959)
¹³ R. B. Laughlin, Phys. Rev. Lett. **50**, 1395 (1983)
¹⁴ A.H. MacDonald, G.C. Aers and M.W.C. Dharma-wardana, Phys. Rev. B **31**, 5529 (1985).
¹⁵ P. Gori-Giorgi, S. Moroni, and G.B. Bachelet, Phys. Rev. B **70**, 115102 (2004)
¹⁶ M. W. C. Dharma-wardana and François Perrot, Euro- physics Letters, **63**, 660-666 (2003)
¹⁷ G. S. Atwal, I. G. Khalil and N. W. Ashcroft, Phys. Rev. B, **67** 115107 (2003)
¹⁸ M. W. C. Dharma-wardana and François Perrot, Phys. Rev. B **70**, 035308 (2004)
¹⁹ N. Drummond (private communication). We thank Dr. Niel Drummond for providing us with numerical tabulations of the relevant $g(r)$.
²⁰ M. W. C. Dharma-wardana and François Perrot, Phys. Rev. Lett. **90**, 136601 (2003)
²¹ M. Holzmann, B. Bernu, V. Olevano, R.M. Martin, and D.M. Ceperley, Phys. Rev. B **79**, 041308(R) (2009);